*Supporting information*

# Kinetic Analysis of Ag Particle Redispersion into ZSM-5 in the Presence of Coke Using *In Situ* XAFS

*Kazumasa Murata[a], Junya Ohyama[b, c], Atsushi Satsuma*[a, b]*

[a]Graduate School of Engineering, Nagoya University, Nagoya 464-8603, Japan

[b]Faculty of Advanced Science and Technology, Kumamoto University, Kumamoto 860-8555, Japan

[c]Elements Strategy Initiative for Catalysts and Batteries (ESICB), Kyoto University, Katsura, Kyoto 615-8520, Japan

Corresponding Author

*E-mail: satsuma@chembio.nagoya-u.ac.jp.

**Table S1.** Structural properties of the H-ZSM-5 and Ag-ZSM-5 (Ag/Al = 0.37) obtained from $N_2$ adsorption-desorption isotherms

| Samples | $S_{BET}$[a] ($m^2\ g^{-1}$) | $S_{External}$[b] ($cm^2\ g^{-1}$) | $V_{micro}$[c] ($cm^3\ g^{-1}$) |
|---|---|---|---|
| H-ZSM-5-AP | 397 | 2 | 0.17 |
| Ag-ZSM-5-AP | 352 | 1 | 0.15 |
| Ag-ZSM-5-AA | 16 | 2 | 0.01 |
| Ag-ZSM-5-AR | 358 | 1 | 0.16 |

[a]BET surface area. [b]External surface area determined by t-plot. [c]Micropore volume determined by t-plot.

**Table S2.** Rate constants of the redispersion of Ag particles in Ag-ZSM-5 measured under various conditions

| Experimental conditions | | Rate constant $k_1$ ($\times 10^{-2}\ min^{-1}$) | $t_{offset}$ (min) |
|---|---|---|---|
| Temperature (°C) | $O_2$ concentration (%) | | |
| 450 | 10 | 0.16±0.00 | 67 |
| 500 | 10 | 0.66±0.00 | 26 |
| 550 | 10 | 1.71±0.02 | 12 |
| 600 | 10 | 6.57±0.09 | 4 |
| 600 | 5 | 2.57±0.03 | 8 |
| 600 | 15 | 12.25±0.23 | 3 |

**Table S3.** Comparison of rate constant for the redispersion of Ag particles in Ag-ZSM-5 with and without coke

| Ag-ZSM-5 samples | Rate constant $k_1$ ($\times 10^{-2}\ min^{-1}$) | $t_{offset}$ (min) |
|---|---|---|
| Ag-ZSM-5-AA (with coke) | 6.57±0.09 | 4 |
| Ag-ZSM-5-AH (without coke) | 6.56±0.32 | 1 |

**Table S4.** Raman band assignments of coke species[1–3]

| Raman shift ($cm^{-1}$) | Raman band assignments |
|---|---|
| 1610 | C=C stretch of monomeric or polycyclic aromatic hydrocarbons |
| 1546 | C=C stretches of conjugated olefins |
| 1462, 1421 | C=C stretch of cyclopentadienyl species |
| 1377 | C−H bending or aromatic ring breathing vibrations |
| 1180 | $CH_2$ twisting vibrations |

**Table S5.** Rate constants of coke combustion in Ag-ZSM-5 measured under various conditions

| Experimental conditions | | Rate constant $k_2$ ($\times 10^{-2}$ $min^{-1}$) | $t_{offset}$ (min) |
|---|---|---|---|
| Temperature (°C) | $O_2$ concentration (%) | | |
| 400 | 10 | 0.03±0.00 | 60.0 |
| 450 | 10 | 0.05±0.00 | 60.0 |
| 500 | 10 | 1.15±0.00 | 22.6 |
| 550 | 10 | 4.74±0.02 | 5.6 |
| 600 | 10 | 7.81±0.08 | 5.9 |
| 600 | 1 | 1.28±0.00 | 17.6 |
| 600 | 5 | 2.32±0.02 | 18.3 |
| 600 | 15 | 10.55±0.12 | 4.9 |

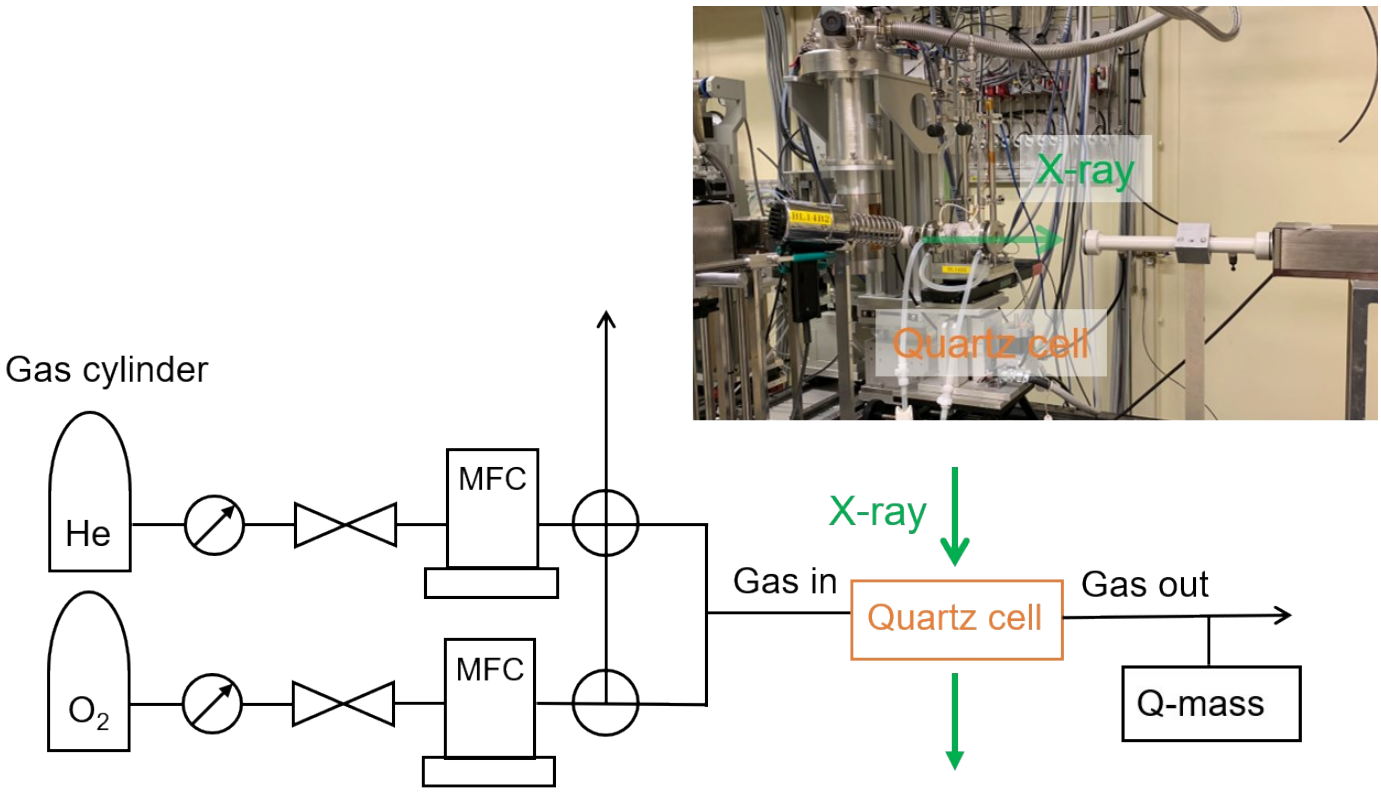


**Figure S1.** Schematic illustration of experimental apparatus for *in situ* XAFS measurements.

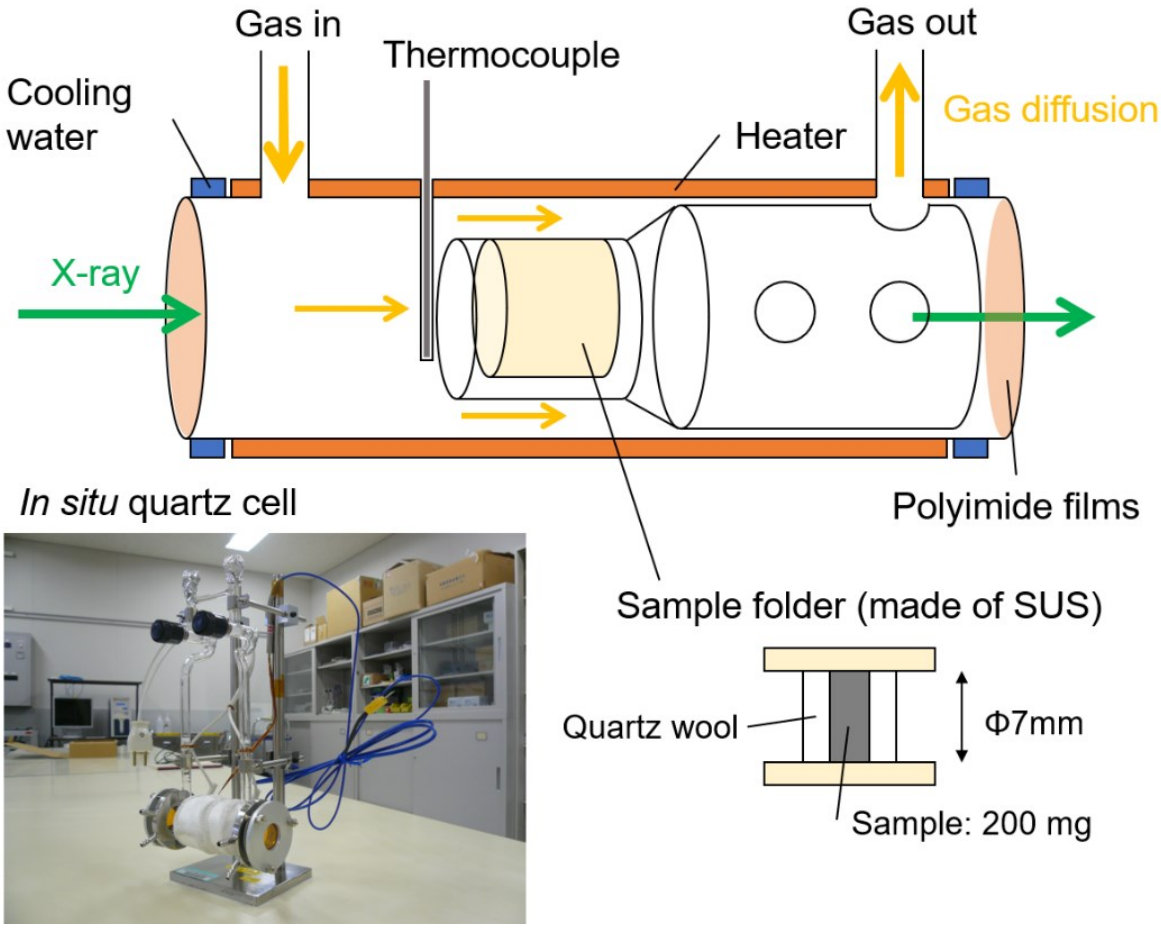


**Figure S2.** Schematic illustration of *in situ* quartz cell.

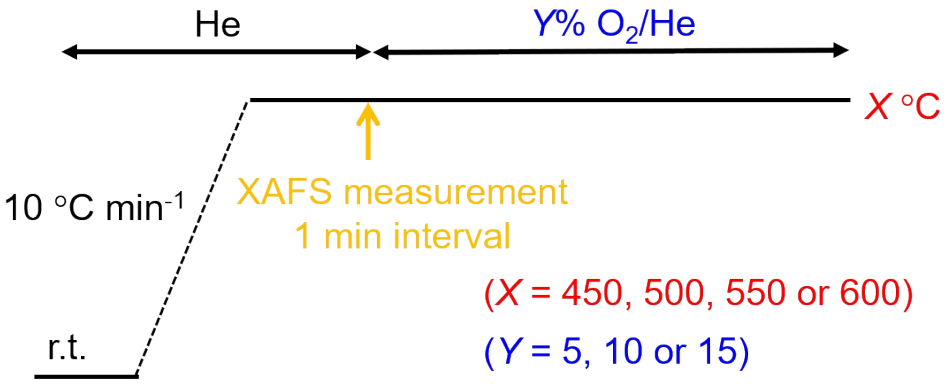


**Figure S3.** Experimental procedure of *in situ* XAFS measurements for the redispersion of Ag particles on Ag-ZSM-5.

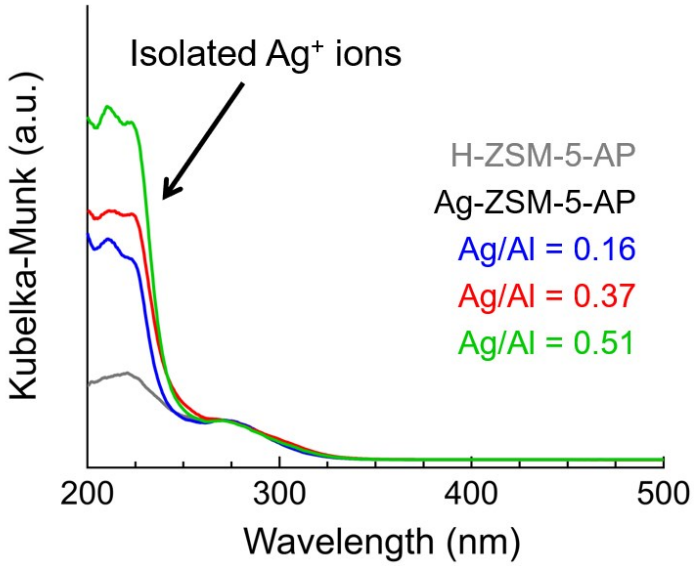


**Figure S4.** UV-vis spectra of H-ZSM-5-AP and Ag-ZSM-5-AP samples with various Ag/Al ratios. UV-vis measurements were performed using a JASCO V-770ICO instrument (JASCO Co.). UV-vis spectra were obtained at room temperature and background spectrum was obtained using $Ba(SO_4)$ powder. UV-vis bands in range of 200–250, 250–330, and 330–500 nm were assigned to isolated Ag+ ions, small $Ag_n^{\delta+}$ ($n \leq 4$) clusters, and larger $Ag_n^{\delta+}$ ($n \leq 8$) clusters or Ag particles, respectively.[1–4]

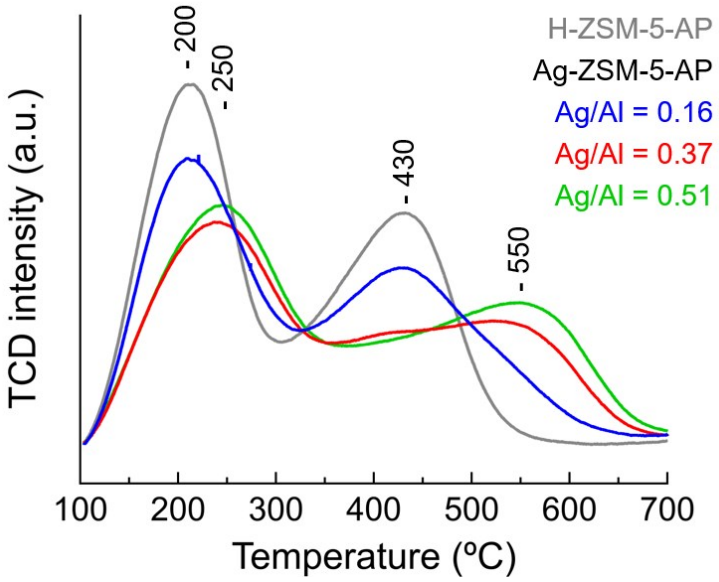


**Figure S5.** $NH_3$-TPD profiles of H-ZSM-5-AP and Ag-ZSM-5-AP samples with various Ag/Al ratios.

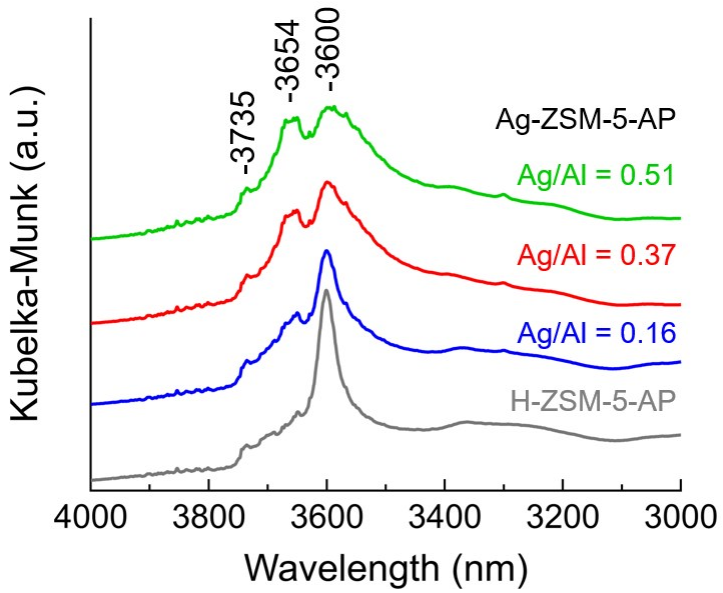


**Figure S6.** IR spectra of H-ZSM-5-AP and Ag-ZSM-5-AP samples with various Ag/Al ratios pretreated under 10% $O_2$/Ar at 600 °C. FT-IR measurements were performed using a JASCO FT/IR-6600 instrument (JASCO Co.) with a liquid-nitrogen-cooled HgCdTe (MCT) detector. IR spectra were obtained at 300 °C and background spectrum was obtained using KBr powder.

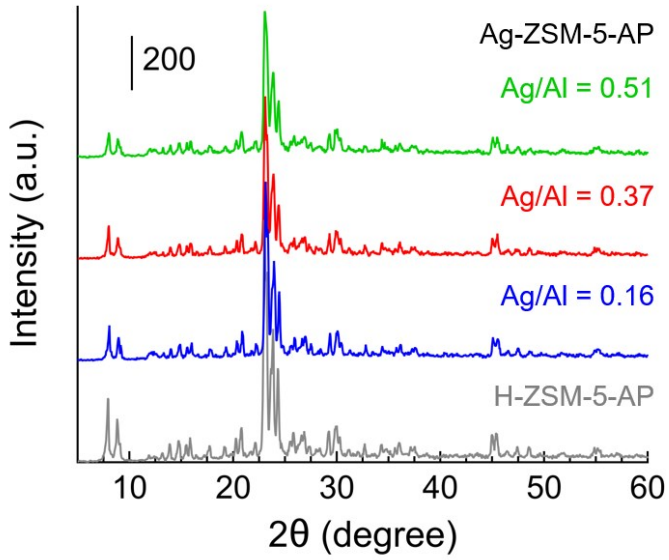


**Figure S7.** XRD patterns of H-ZSM-5-AP and Ag-ZSM-5-AP with various Ag/Al ratios. The diffraction patterns of Ag metal[5,6] at 38.2 and 44.4°, and AgO[7] at 32.6 and 46.2° were not detected.

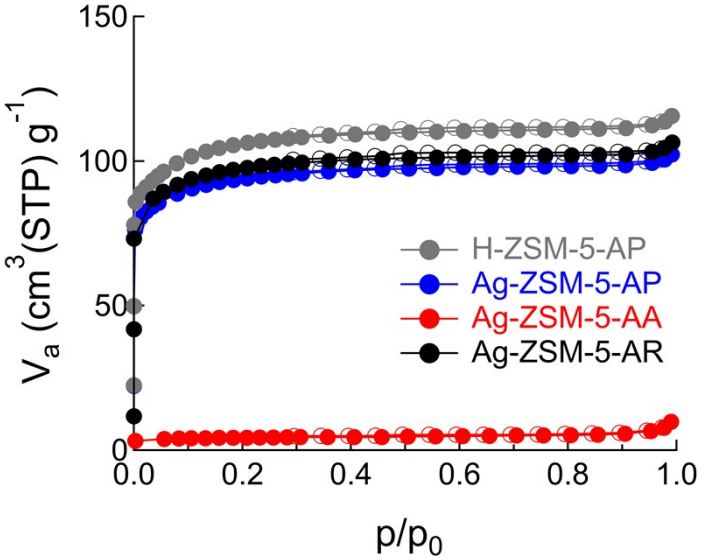


**Figure S8.** $N_2$ adsorption−desorption isotherms of H-ZSM-5 and Ag-ZSM-5 (Ag/Al = 0.37) samples. $N_2$ adsorption−desorption were conducted on a volumetric adsorption instrument (MicrotracBEL, BELSORPminiII) at liquid nitrogen temperature. The samples were pretreated at 120 °C under vacuum for 1 h.

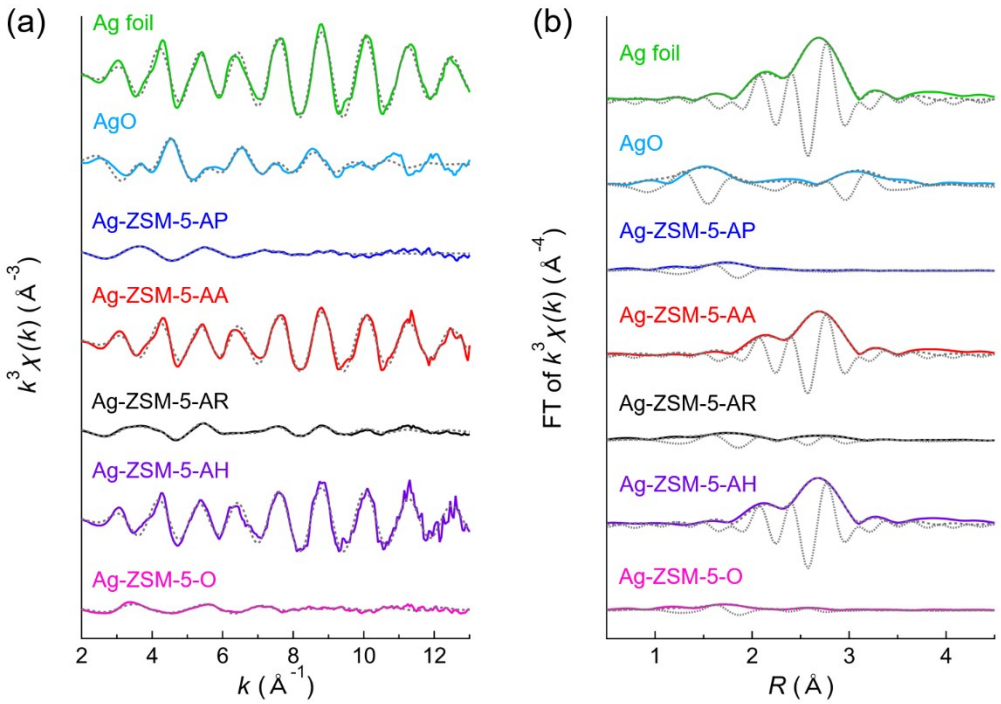


**Figure S9.** Ag K-edge (a) $k^3$-weighted EXAFS and (b) FTs of EXAFS spectra for various Ag-ZSM-5 (solid lines: raw data; broken lines: fitting data, dot lines: imaginary component of fitting data).

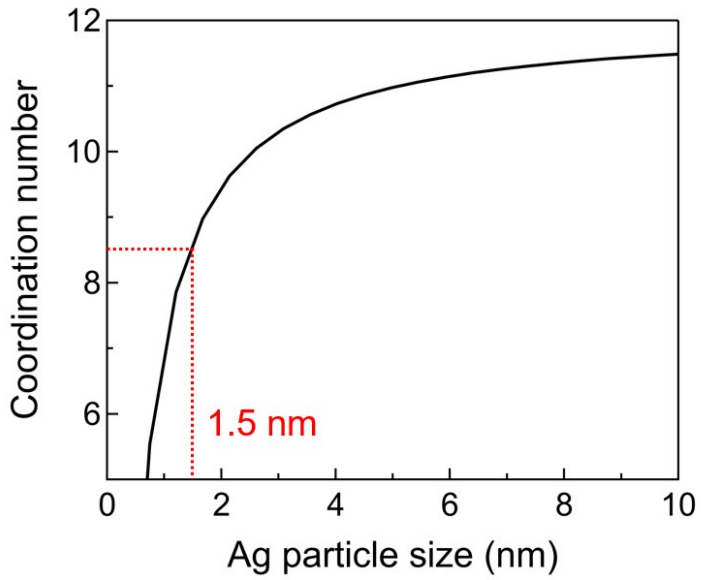


**Figure S10.** Correlation of Ag particle size with average coordination number assuming a fcc cubo-octahedron shape.

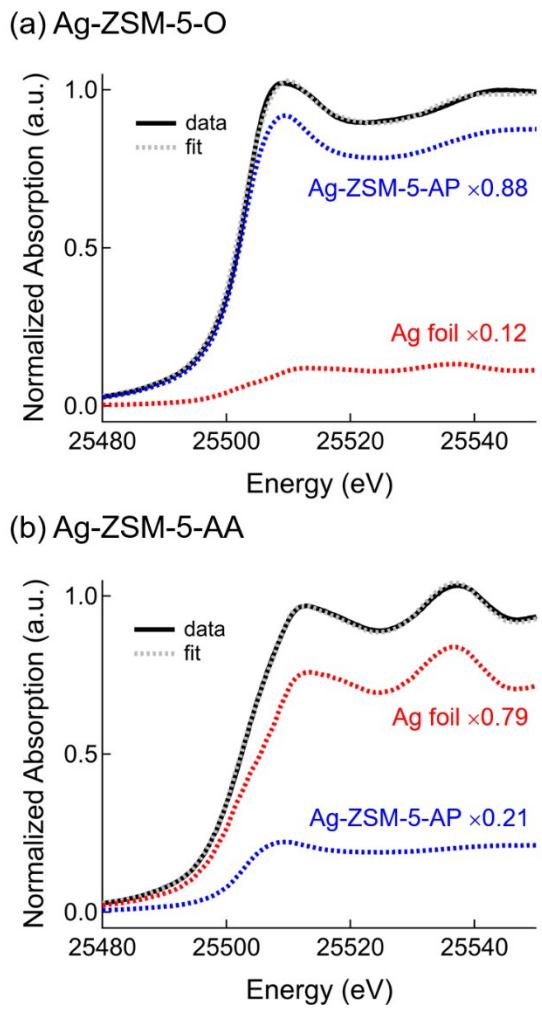


**Figure S11.** LCF results of Ag K-edge XANES spectra, which were measured at room temperature, of (a) Ag-ZSM-5-AP (Ag/Al = 0.37) pretreated under 10% $O_2$/He at 600 °C and (b) Ag-ZSM-5-AA (Ag/Al = 0.37) pretreated under He at 600 °C (solid lines: raw data; dot lines: fitting data). Ag foil and Ag-ZSM-5-AP, which were measured at room temperature, were defined as LCF reference of [$Ag^0$] = 1 and 0, respectively.

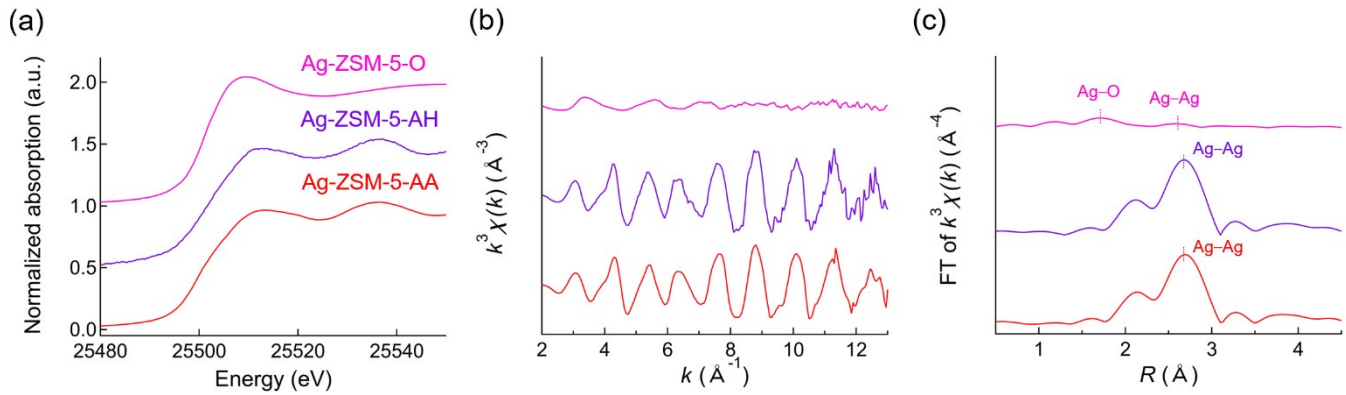


**Figure S12.** Ag K-edge (a) XANES, (b) $k^3$-weighted EXAFS, and (c) FT-EXAFS spectra for Ag-ZSM-5-O (pink line), Ag-ZSM-5-AH (purple line), and Ag-ZSM-5-AA (red line) with Ag/Al = 0.37. The FT range in k space: 3.0–11.0 $Å^{-1}$.

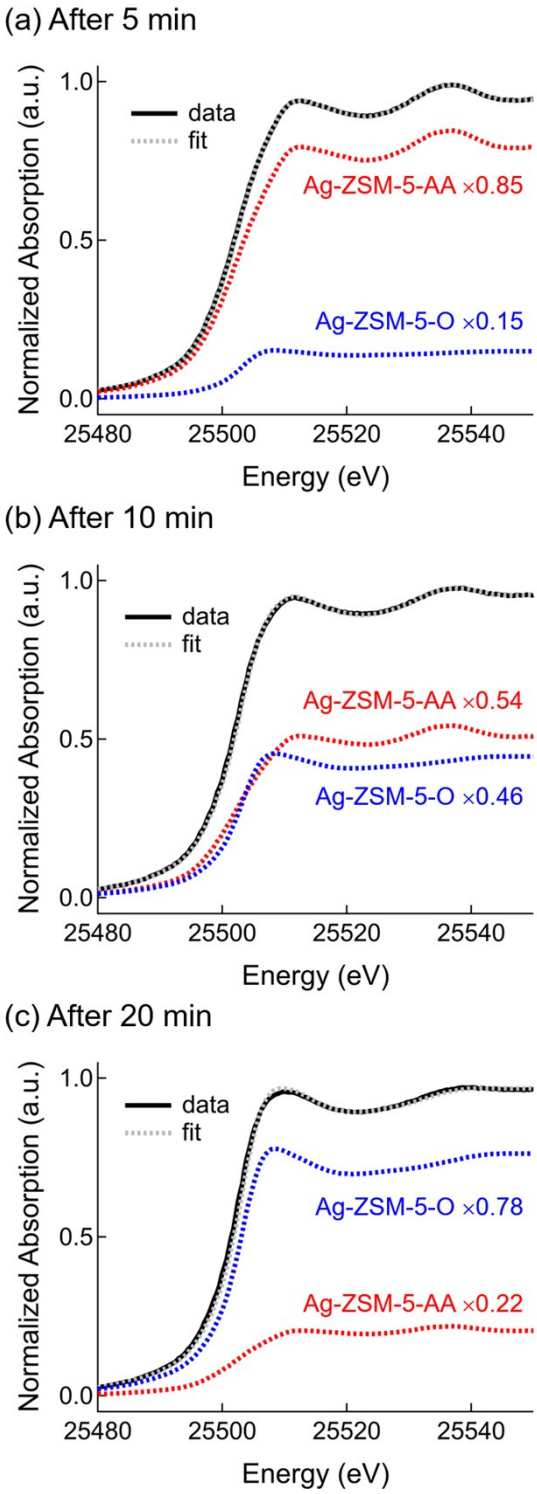


**Figure S13.** LCF results of Ag K-edge XANES spectra of Ag-ZSM-5-AA (Ag/Al = 0.37) at (a) 5, (b) 10, and (c) 20 min after introducing of a flowing of 10% $O_2$/He at 600 °C (solid lines: raw data; dot lines: fitting data). Ag-ZSM-5-AA and Ag-ZSM-5-AP, which were measured at 600 °C, were defined as LCF reference of [$Ag^0$] = 0.79 and 0.12 ([$Ag^+$] = 0.21 and 0.88), respectively.

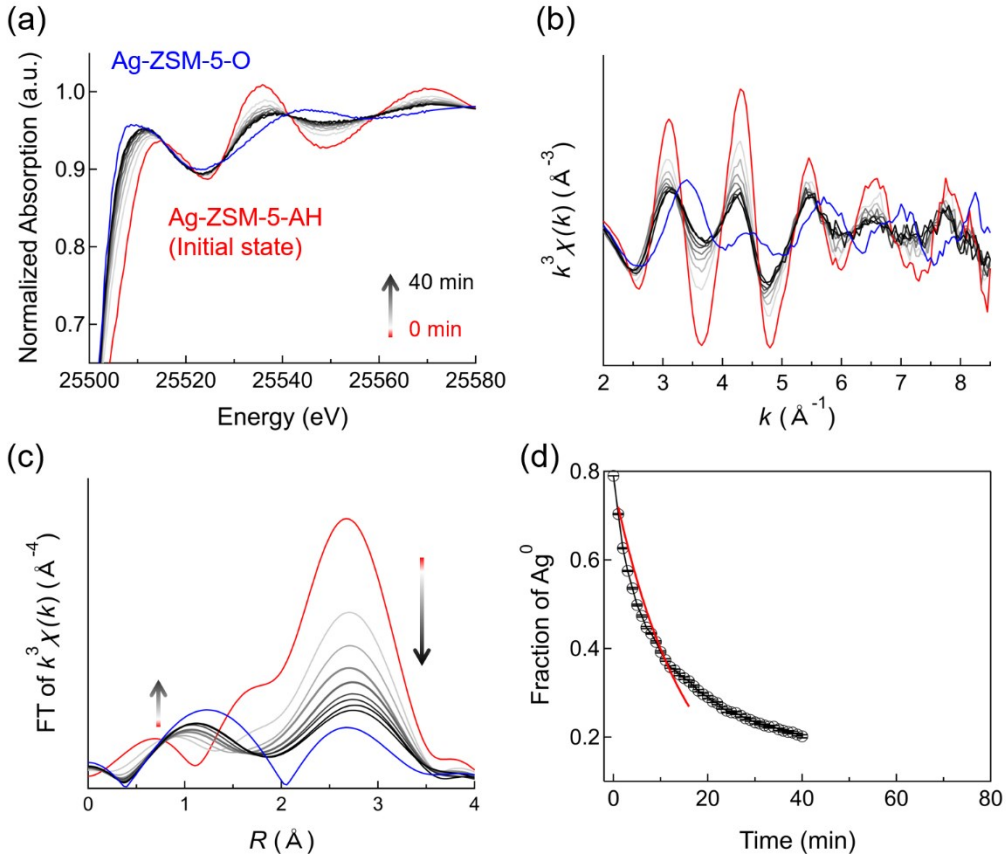


**Figure S14.** Series of Ag K-edge (a) XANES, (b) $k^3$-weighted EXAFS, and (c) FT-EXAFS spectra for the Ag-ZSM-5-AH under a flowing of 10% $O_2$/He at 600 °C, which were measured for 40 min. (d) Time course of $Ag^0$ fraction determined by LCF for a series of Ag K-edge XANES spectra. Red line indicates fitting result by pseudo-first-order kinetic model.

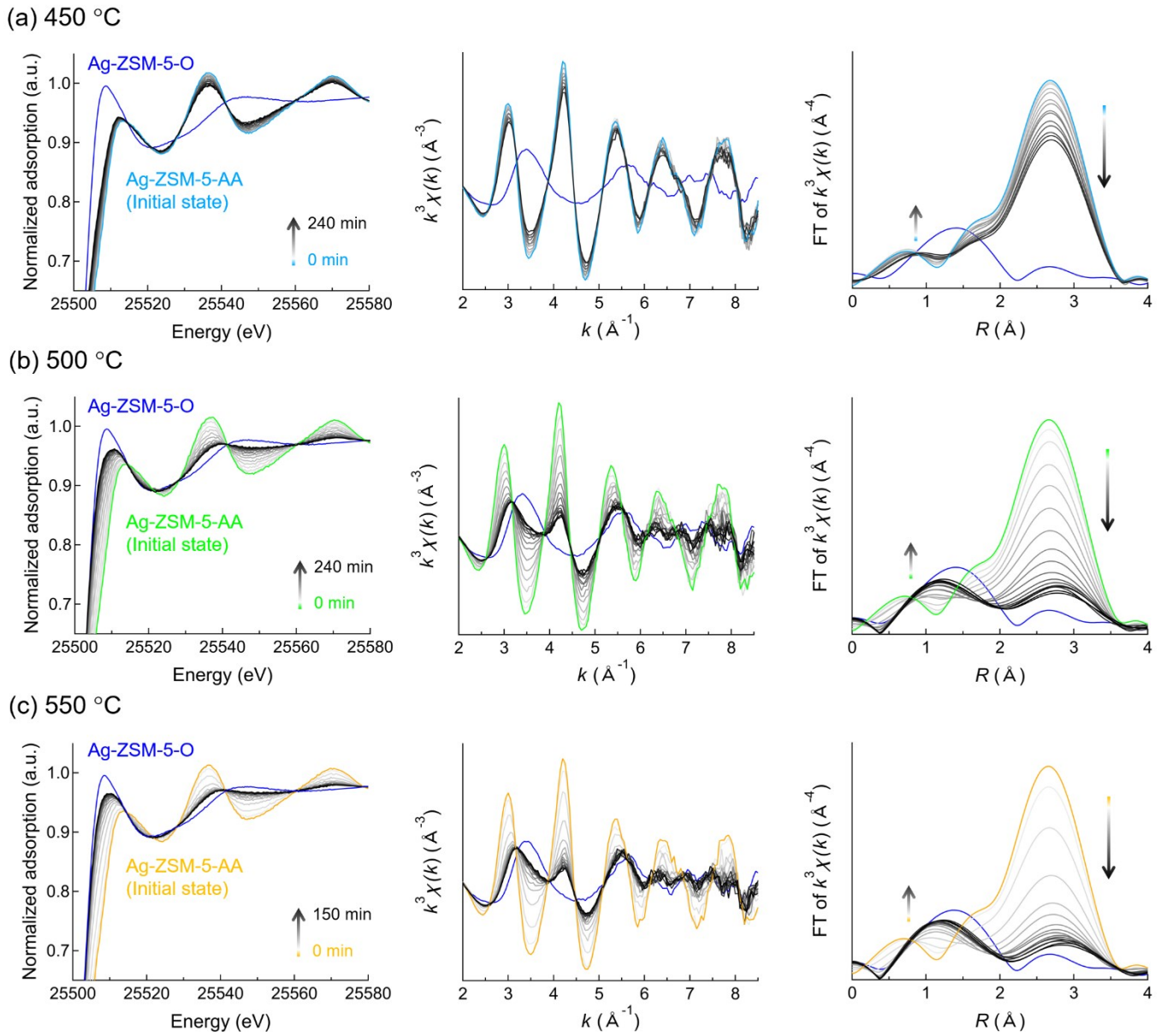


**Figure S15.** Series of Ag K-edge XANES, $k^3$-weighted EXAFS, and FT-EXAFS spectra for the Ag-ZSM-5-AA under a flowing of 10% $O_2$/He at various temperature ((a) 450 °C (b) 500 °C, and (c) 550 °C), together with XANES and FT-EXAFS spectra of Ag-ZSM-5-AP as references.

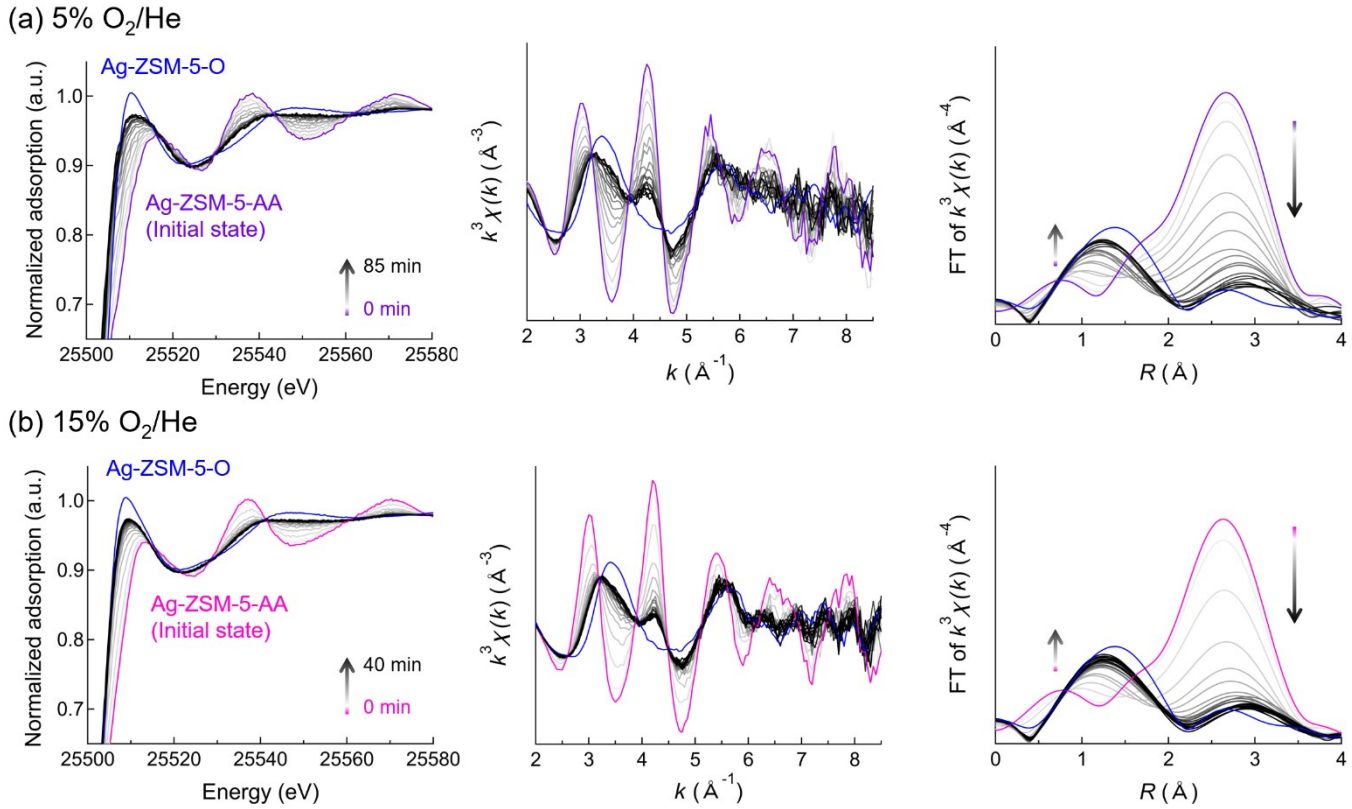


**Figure S16.** Series of Ag K-edge XANES, $k^3$-weighted EXAFS and FT-EXAFS spectra for the Ag-ZSM-5-AA under a flowing of (a) 5% and (b) 15% $O_2$/He at 600 °C, together with XANES and FT-EXAFS spectra of Ag-ZSM-5-AP as references.

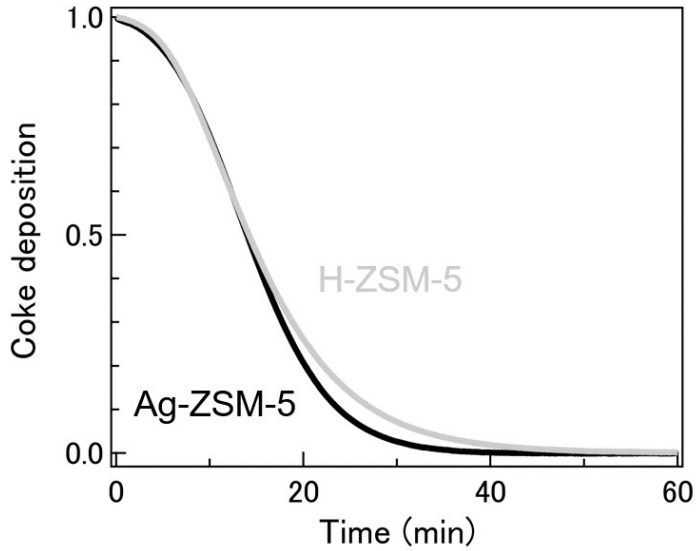


**Figure S17.** Comparison of behaviors of coke combustion in H-ZSM-5-AA and Ag-ZSM-5-AA, which were measured at 600 °C under 10% $O_2$/Ar.

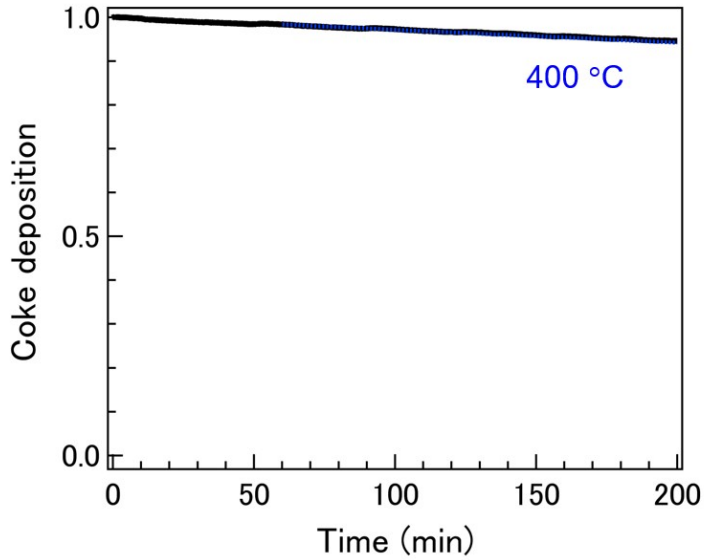


**Figure S18.** Behaviors of coke combustion in the Ag-ZSM-5-AA measured at 400 °C under 10% $O_2$/Ar.

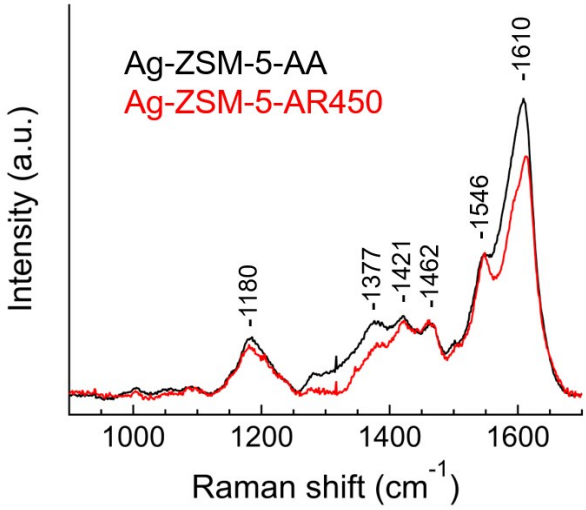


**Figure S19.** Raman spectra of (a) Ag-ZSM-5-AA and (b) Ag-ZSM-5-AR450 (Ag/Al = 0.37) in the region of coke species. The Raman spectra were obtained by a JASCO RMP-330 with a Peltier cooled charge coupled device (CCD) detector using a visible laser (λ = 532 nm).

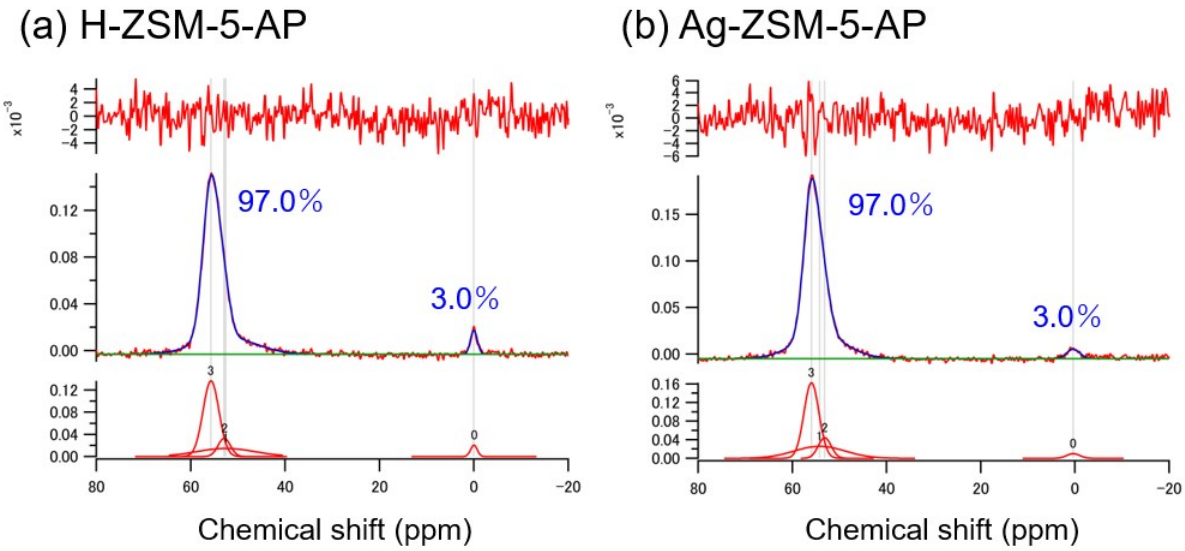


**Figure S20.** (Middle) $^{27}$Al MAS NMR spectra of H-ZSM-5-AP and Ag-ZSM-5-AP (Ag/Al = 0.37), together with Gaussian fitting results. (Top) fitting error and (bottom) each fitted Gaussian peak. Asymmetric NMR peaks were fitted using two or more Gaussian peaks because $^{27}$Al have quadrupole moment and Al atoms in ZSM-5 were slightly different.

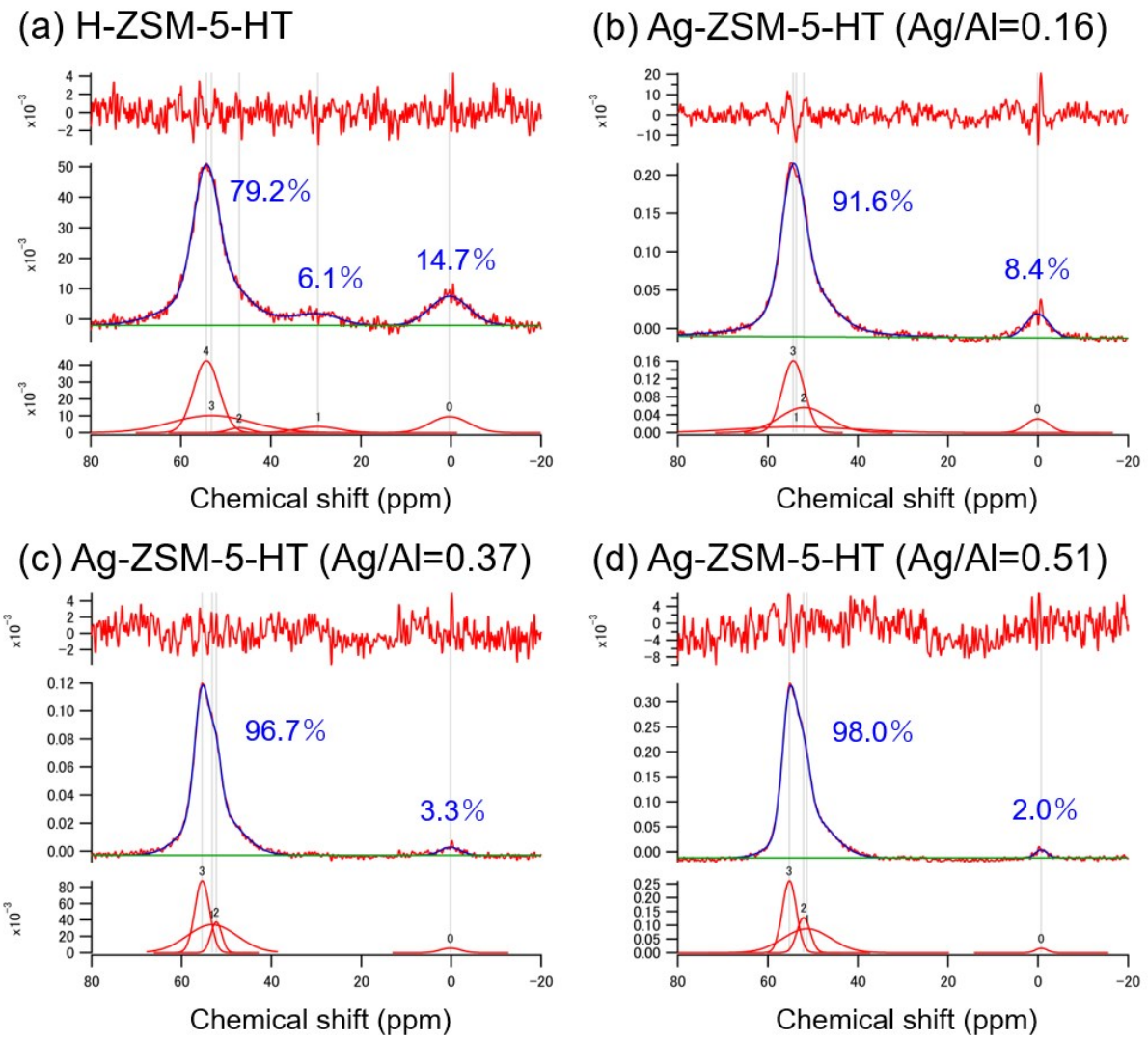


**Figure S21.** (middle) $^{27}$Al MAS NMR spectra of H-ZSM-5-HT and Ag-ZSM-5-HT with various Ag/Al ratio, together with Gaussian fitting results. (top) fitting error and (bottom) each fitted Gaussian peak. Asymmetric NMR peaks were fitted using two or more Gaussian peaks because $^{27}$Al have quadrupole moment and Al atoms in ZSM-5 were slightly different.

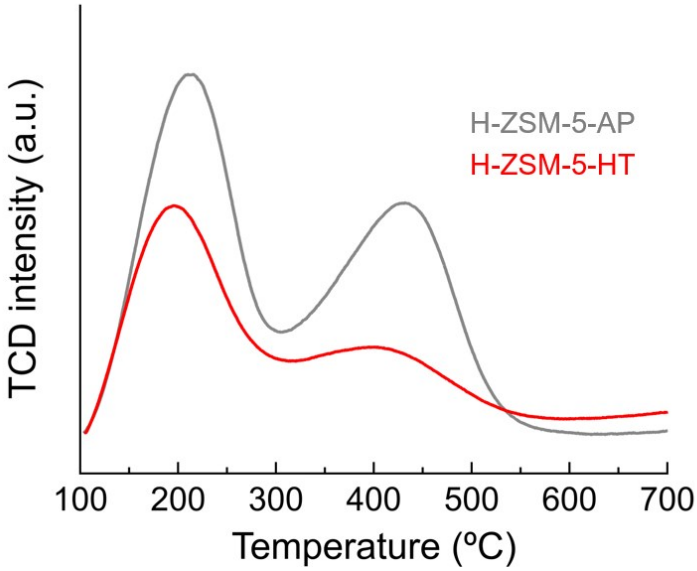


**Figure S22.** $NH_3$-TPD profile of H-ZSM-5-AP and H-ZSM-5-HT.

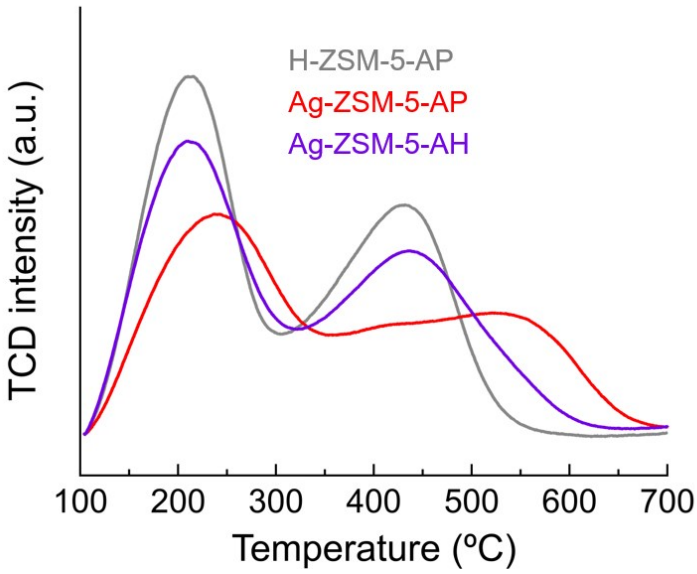


**Figure S23.** $NH_3$-TPD profile of Ag-ZSM-5-AH, together with $NH_3$-TPD profiles of H-ZSM-5-AP and Ag-ZSM-5-AP as references.

## References


1 T. Yumura, A. Oda, H. Torigoe, A. Itadani, Y. Kuroda, T. Wakasugi and H. Kobayashi, *J. Phys. Chem. C*, 2014, **118**, 23874–23887.

2 K. I. Shimizu, K. Sugino, K. Kato, S. Yokota, K. Okumura and A. Satsuma, *J. Phys. Chem. C*, 2007, **111**, 1683–1688.

3 W.-S. Ju, M. Matsuoka, K. Iino, H. Yamashita and M. Anpo, *J. Phys. Chem. B*, 2004, **108**, 2128–2133.

4 J. Shibata, K. I. Shimizu, Y. Takada, A. Shichi, H. Yoshida, S. Satokawa, A. Satsuma and T. Hattori, *J. Catal.*, 2004, **227**, 367–374.

5 F. Wang, J. Ma, G. He, M. Chen, C. Zhang and H. He, *ACS Catal.*, 2018, **8**, 2670–2682.

6 Z. Huang, J. Zhang, Y. Du, Y. Zhang, X. Wu and G. Jing, *ChemCatChem*, 2019, 561–568.

7 B. Gauri, K. Vidya, D. Sharada and W. Shobha, *Res. J. Chem. Environ.*, 2016, **20**, 1–5.